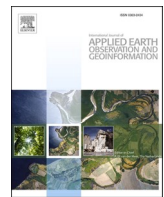




Contents lists available at ScienceDirect

International Journal of Applied Earth Observations and Geoinformation

journal homepage: www.elsevier.com/locate/jag



Climatic factors dominate the spatial patterns of urban green space coverage in the contiguous United States

Conghong Huang^a, Nan Xu^{b,*}

^a Department of Epidemiology and Environmental Health, School of Public Health and Health Professions, University at Buffalo, Buffalo, NY 14214, USA

^b School of Earth Sciences and Engineering, Hohai University, Nanjing 210098, China



ARTICLE INFO

Keywords:

Green spaces mapping
High-resolution imagery
Influencing factors
Spatial pattern
US cities

ABSTRACT

Urban green space (UGS) is directly or indirectly related to the human well-being of urban inhabitants, information on the availability or quantity of UGS is thus very fundamental for policy-makers to conduct sustainable land management. Analysis of UGS patterns and their influencing factors at large scales using high-resolution remotely sensed imagery is still understudied. Our study aimed to map the spatial patterns of UGS coverage (UGSC) in all (i.e., 3,535) urban areas of the contiguous US (CONUS) and uncover the main influencing factors that dominate the spatial patterns. We mapped the UGS cover of each urban area using the one-meter high-resolution remote sensing images provided by the National Agriculture Imagery Program (NAIP) of the US on the Google Earth Engine platform. Then we calculated the UGSC of each urban area and quantified the spatial patterns of UGSC for the CONUS urban areas. We established a random forests model to quantify the impact of the influencing factors on UGSC. The results showed that: (1) UGSC in the CONUS urban areas varied largely from 2.2% in Kayenta, AZ to 89.36% in Ocala Estates, FL, with a mean UGSC of 39.43% (SD = 18.19%); (2) UGSC in humid Eastern US was much higher than that in urban areas with hyper-arid or arid climate classes in Western or Central regions of the US. Yet, UGSC of urban areas with different city sizes dose not vary largely; (3) the climatic factors were the main influencing factors that dominate the spatial patterns of UGSC in urban areas of the CONUS, while the socio-economic and terrain factors play relatively less important roles in shaping the UGSC pattern.

1. Introduction

Urban green space (UGS) can benefit urban residents by providing multiple ecosystem services. For example, UGS can mitigate urban heat island effects (Sebastiani et al., 2021), remove air pollutants (Jaung et al., 2020), and provide recreational services (Massoni et al., 2018). In addition, UGS has been demonstrated to be associated with multiple health benefits (Reid et al., 2017). Specifically, previous studies have found that living near UGS is associated with lower mortality risk (Astell-Burt et al., 2021; Bauwelinck et al., 2021), reduced depression and anxiety (Hystad et al., 2019), and improved self-reported health (Jarvis et al., 2020). Thus, as an important component of urban ecosystems, UGS is directly or indirectly related to the human well-being of urban residents. As a result, information on availability or quantity of UGS and their spatial patterns are thus very fundamental for policy-makers to conduct sustainable land management, and mapping and quantifying UGS have drawn much attention in the past decades.

Mapping and quantifying UGS at multiple scales (e.g., city scale, regional scale, and country scale) have been made in previous studies using various remote sensing data sources. Many previous studies have used medium resolution remote sensing data for UGS mapping, especially for large-scale studies as the free or low costs of medium resolution satellite data. For example, the 30 m Landsat satellite data were frequently applied for mapping urban land cover and UGS of world cities (Corbane et al., 2020; Dobbs et al., 2017; Huang et al., 2017; Kuang, 2019; Richards and Belcher, 2020). Although the medium resolution satellite data have been widely used in UGS mapping, the drawback of mixture pixels in the medium resolution satellite data in urban mapping should be noted because relative coarse resolution remote sensing images may not be ideal to reflect the spatial details of UGS. Some studies have attempted to solve the mixture pixel problem of the medium resolution satellite images through unmixing techniques (Schug et al., 2020). These studies are useful in estimating the ratio of vegetation in each pixel when high resolution satellite images are not available, while

* Corresponding author.

E-mail address: hhuxunan@gmail.com (N. Xu).

<https://doi.org/10.1016/j.jag.2022.102691>

Received 1 December 2021; Received in revised form 10 January 2022; Accepted 18 January 2022

Available online 3 February 2022

1569-8432/© 2022 The Authors.

Published by Elsevier B.V. This is an open access article under the CC BY-NC-ND license

(<http://creativecommons.org/licenses/by-nc-nd/4.0/>).

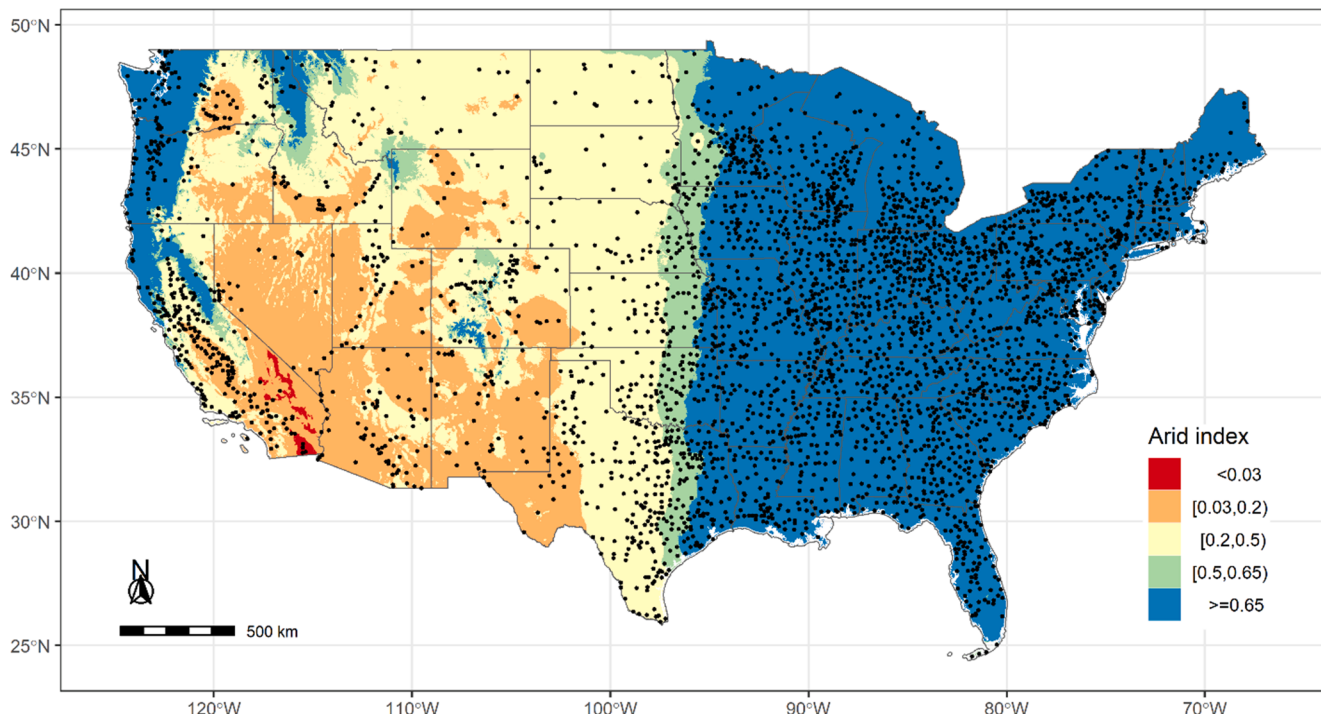


Fig. 1. Locations (black dots) of each urban area in the contiguous US with a base map is the arid index map obtained from the Global Aridity and PET Product (Trabucco and Zomer, 2018; Zomer et al., 2008). The five categories of arid index represent hyper arid (<0.03), arid (0.03–0.2), semi-arid (0.2–0.5), dry sub-humid (0.5–0.65), and humid climate (>0.65), respectively.

it is not ideal for mapping vegetation cover precisely with medium resolution satellite images, especially for heterogeneous urban landscapes. To overcome this drawback, some studies adopted high-resolution remote sensing images for UGS mapping (Kuklina et al., 2021; Qian et al., 2015; Sulma et al., 2016; Vigneshwaran and Vasantha Kumar, 2019; Zhou et al., 2018). The above-mentioned studies that used high-resolution remotely sensed imagery were mainly performed at city scales as the high costs for purchasing the high-resolution remote sensing data. Fortunately, some programs released high-resolution remote sensing data that cover large areas for public use with no costs in recent years. For example, the National Agriculture Imagery Program (NAIP) of the United States (US) provides 1-meter resolution remote sensing data for the continental US. Such programs have provided promising ways for mapping large-scale UGS at a very high resolution.

Moreover, analyzing various influencing factors of UGS patterns from regional to global scales has also drawn much attention to the UGS studies (Yang et al., 2014). Previous studies mainly consider climatic (e.g., precipitation) and terrain data (e.g., mean elevation) as natural factors that may affect UGS distribution, and population (e.g., population density) and wealth (e.g., per capita GDP) data are frequently used as socio-economic factors (Dobbs et al., 2017; Fuller and Gaston, 2009; Zhao et al., 2013).

Though many efforts have been made on the spatial pattern of UGS and their influencing factors, there are still several aspects that are less considered in previous studies. Firstly, many studies focused on major or sampled cities in their countries, while few studies take all their cities that include both small and large cities at a large scale (e.g., country scale) for analysis. Secondly, many large-scale UGS studies used medium resolution remote sensing data (mainly Landsat data) for their analysis, while few studies used high-resolution remote sensing data for large-scale UGS studies. Lastly, although some influencing factors have been shown to be associated with UGS pattern, the major or relative importance of factors on shaping the UGS pattern is poorly understood.

The goal of our study is to reveal the spatial patterns of UGS in all (i.e., 3,535) urban areas of the contiguous US (CONUS) and uncover the

main influencing factors that dominate the spatial patterns. The specific objectives of this study are (1) mapping UGS of each urban area using high-resolution (1 m) remote sensing images; (2) quantifying spatial pattern of UGS distribution for the CONUS urban areas; (3) analyzing influencing factors that dominate the pattern of UGS in the CONUS urban areas.

2. Methods

2.1. Study area

According to the cartographic boundary files of urban areas in 2019 (<https://www.census.gov/geographies/mapping-files/time-series/geo/cartographic-boundary.2019.html>), there are 3,535 urban areas in the CONUS which were delineated with the uniform criteria. All these 3,535 urban areas were selected as our study area (Fig. 1). In total, there are about 0.26 billion population lives in these urban areas. From Fig. 1, we can see that the CONUS exhibits significant spatial variations of urban areas in terms of aridity. Specifically, the humid Eastern US has much denser urban areas than the Western and Central regions of the US.

2.2. Mapping urban green space

In this study, the UGS was defined as tree/shrub cover or grass cover within the boundaries of urban areas (Huang et al., 2021b). We used one-meter high-resolution remote sensing data to map UGS for each urban area in the CONUS. The high-resolution remotely sensed imagery were from the NAIP administered by the USDA's Farm Service Agency (FSA) (<https://www.fsa.usda.gov/programs-and-services/aerial-photography/imagery-programs/naip-imagery/>). The NAIP acquired high-resolution images on a five-year cycle beginning in 2003, and on a three-year cycle since 2009. Google Earth Engine (GEE) platform (Gorelick et al., 2017) has ingested these high-resolution images in their cloud-based geospatial processing platform, and these images are ready

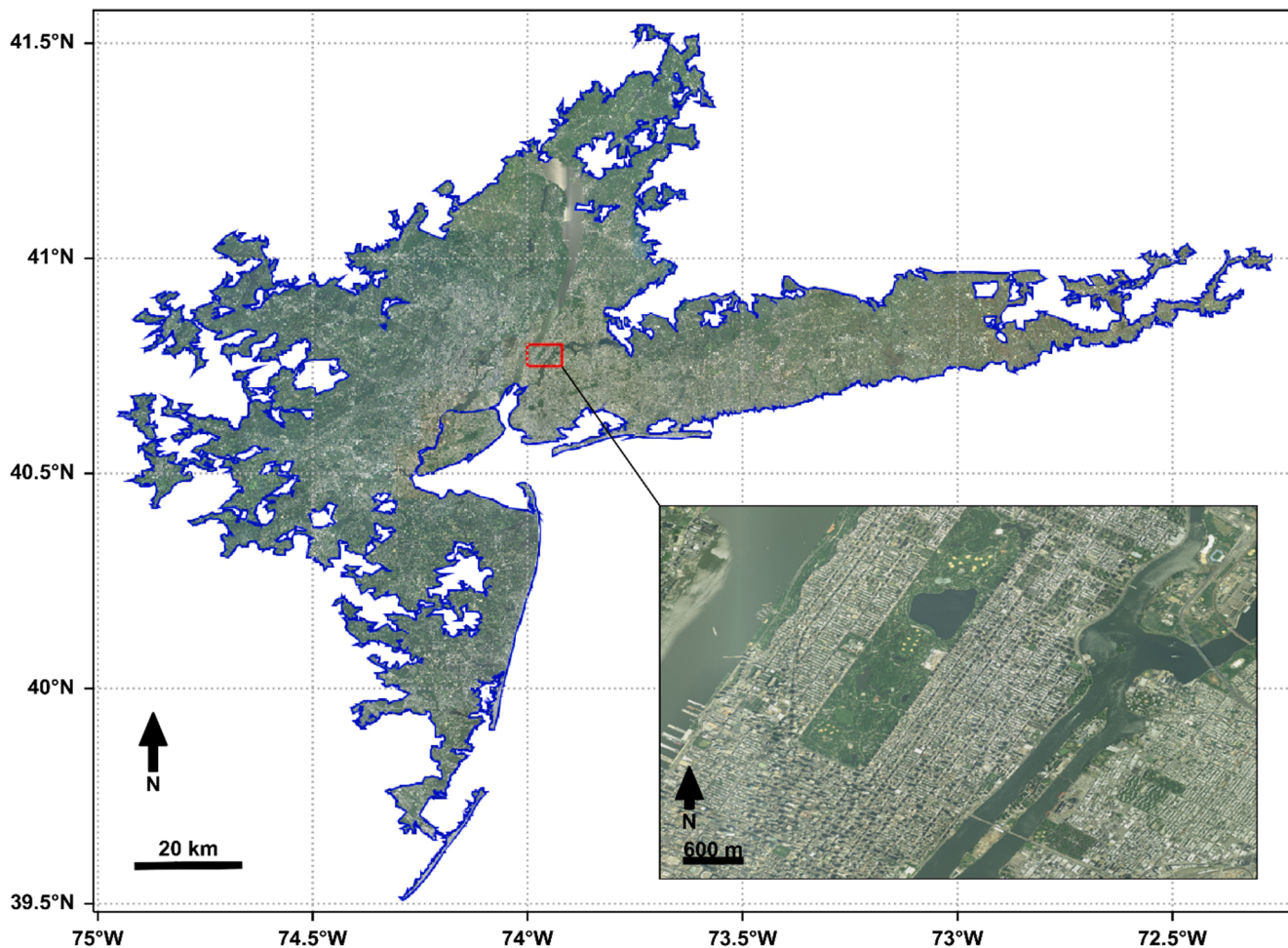


Fig. 2. The true color composited high-resolution remote sensing images (RGB): an example of New York-Newark. The blue polygon represents the boundary of the urban area and the red box demonstrates the remote sensing images in detail in the subset.

to use on the platform without downloading. We mosaiced the latest available cloud-free growing season NAIP images (e.g., 2015–2019) on GEE platform for each urban area. Fig. 2 gives an example of the high-resolution images in the New York-Newark urban area. We then computed the normalized difference vegetation index (NDVI) (Tucker, 1979) based on the NAIP imagery according to the following equation.

We used a threshold of 0.2 (Hashim et al., 2019; Spadoni et al., 2020) to classify NDVI images into vegetation cover ($NDVI \geq 0.2$) and non-vegetation cover ($NDVI < 0.2$). We masked the water surfaces based on the year 2019 global surface water dataset (Pekel et al., 2016). To assess the vegetation cover classification accuracy, we randomly selected 20 urban areas and randomly sampled 50 pixels for each of the 20 urban areas. Then we interpreted these 1000 samples manually by referencing the one-meter high-resolution images. Finally, we calculated the overall accuracy and Kappa coefficient based on the classification and interpreted results. As there are seldom croplands in urban areas of the US, we suppose all the vegetation cover within urban areas that we extracted with the NDVI images are UGS cover. With boundaries and classified vegetation and non-vegetation cover images of each urban area, UGS cover of each urban area was mapped and extracted. We then calculated UGS coverage (UGSC) (Huang et al., 2021b) of each urban area based on the following equation.

$$UGSC = \frac{UGS_{area}}{Urban_{area}} \times 100\% \quad (1)$$

where UGS_{area} indicates the area for each urban green space cover, and $Urban_{area}$ indicates the area for each urban area.

2.3. Analyzing the influencing factors of urban green space coverage

To analyze influencing factors that dominate the spatial pattern of UGSC in the CONUS, we collected variables data to reflect natural (i.e., climatic and terrain) and socio-economic factors that may have a potential effect on the UGSC spatial distribution. We obtained 19 bioclimatic variables according to the WorldClim database (Fick and Hijmans, 2017), and aridity index and potential evapotranspiration data from the Global Aridity and PET Database (Trabucco and Zomer, 2018; Zomer et al., 2008) to reflect climatic conditions of each urban area in the CONUS. The mean values of the bioclimatic variables, aridity index and potential evapotranspiration of each urban area were calculated by aggregating pixels mean of the raster data. We calculated mean elevation and mean slope based on the Shuttle Radar Topography Mission (SRTM) digital elevation product (Jarvis et al., 2008) to reflect the terrain conditions of each urban area. We calculated or collected the area of urban areas, total population, population density, per capita income, and mean nighttime light intensity (NTLI) to reflect socio-economic conditions of each urban area in the CONUS. The total population and per capita income data were obtained from the website of the Census Bureau of the US (<https://data.census.gov/cedsci/>). The mean NTLI for each urban area was computed via the Visible Infrared Imaging Radiometer Suite (VIIRS) Day/Night Band (DNB) nighttime data (Mills et al., 2013). The annual mean NTLI in 2019 was calculated based on the monthly VIIRS nighttime data. Then the mean NTLI for each urban area was computed by aggregating pixels mean of the composited annual mean NTLI data.

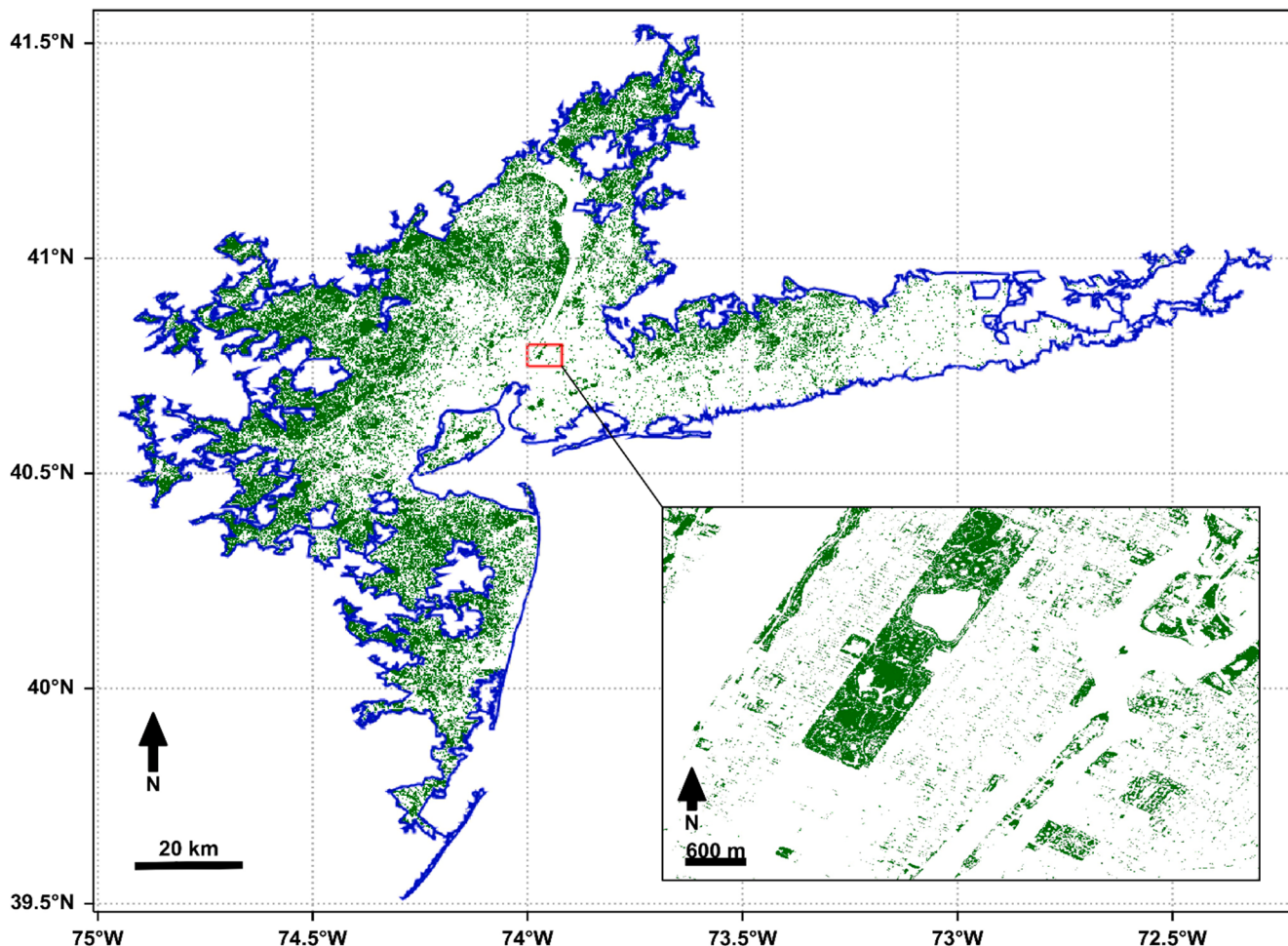


Fig. 3. Mapped urban green spaces cover (pixels in green color) using high-resolution images: an example of the New York-Newark urban area. The blue polygon represents the boundary of the urban area and the red box demonstrates the mapped urban green spaces cover in detail in the subset.

We constructed a random forests (RF) (Breiman, 2001) regression model to quantify the impact of the 28 potential influencing factors on UGSC using the ranger package (Wright and Ziegler, 2017) in R (version 3.5.3). The number of trees parameter of the RF model was set to 500. The number of variables to possibly split at each node parameter was set to the square root of the number of variables. The variable importance mode parameter was set as ‘Impurity’. We also set the seed parameter as a number of 123,456,789 to make the RF model reproducible. We chose the RF algorithm as it is a non-linear regression algorithm that can handle complex relationships between the influencing factors and UGSC. We used 10-fold cross-validation (CV) method (Huang et al., 2021a) based on the urban areas to assess the RF model performance. We also reported the relative importance of each variable based on the RF modeling results that can be used to discover the major influencing factors that dominate the spatial patterns of UGSC in urban areas of the CONUS.

3. Results

3.1. Spatial patterns of urban green space in the contiguous US

The vegetation cover classification accuracy assessment results showed that we achieved an overall accuracy of 95.5% and a Kappa coefficient of 0.91. For each urban area, we generated UGS cover maps (taking the New York-Newark urban area as an example in Fig. 3) and calculated UGSC. Fig. 4 shows the UGSC of each urban area in the CONUS. The UGSC of urban areas is distributed unevenly across the

CONUS with the obvious spatial pattern. To be specific, it varied largely from 2.2% in Kayenta, AZ to 89.36% in Ocala Estates, FL, with a mean UGSC of 39.43% ($SD = 18.19\%$). About 15% of the 3,535 urban areas have their UGSC values larger than 60%, while 17% of the 3,535 urban areas have their UGSC values <20%. Urban areas in Eastern US have higher UGSC than urban areas in the Western and Central US except for urban areas in Northwestern US.

We also calculated mean UGSC of urban areas for all states (Fig. 5). Urban areas in Alabama (AL) have the largest mean UGSC (68.63%), while urban area in Arizona (AZ) has the lowest mean UGSC (12.37%). States in Eastern US also have higher UGSC than states in Western and Central US, which is similar to the spatial pattern of UGSC of all urban areas. Washington (WA) and Oregon (OR) in the Western US have a higher UGSC because they also own many humid areas in the coastal zone.

The UGSC in urban areas of different climate classes varied significantly (Fig. 6a). There is a clear reduction of UGSC from humid regions to hyper-arid regions. The mean UGSC in urban areas of the hyper-arid region is the lowest (11.24%). The mean UGSC in urban areas of humid regions is the highest (45.07%), which is three times higher than that in urban areas of hyper-arid regions. We also divided all the urban areas into eight groups according to their city size (total population). The UGSC of urban areas with different city sizes does not vary largely (Fig. 6b). The UGSC of urban areas with their population between 10,000 and 30,000 is the lowest (38.22%), while the UGSC of urban areas with a population greater than 1,000,000 is the highest (43.49%).

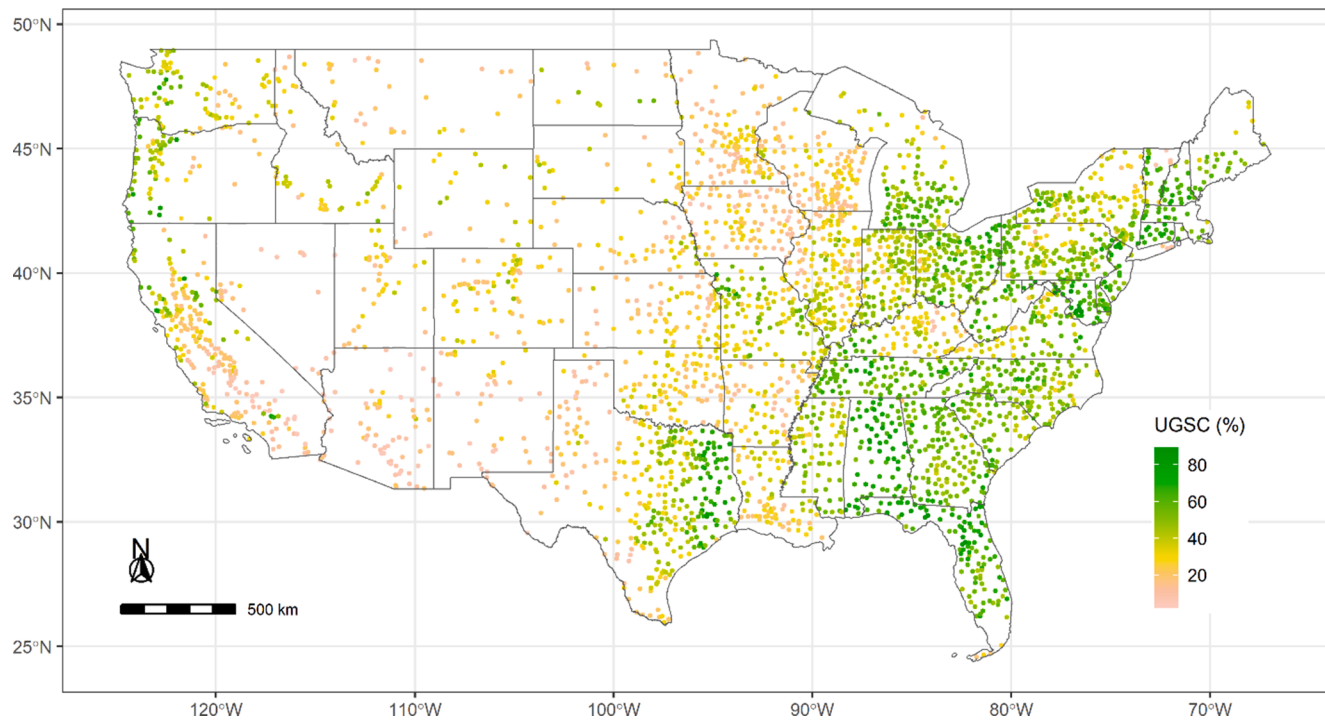


Fig. 4. Spatial pattern of urban green space coverage (UGSC, %) of the 3,535 urban areas in the contiguous United States.

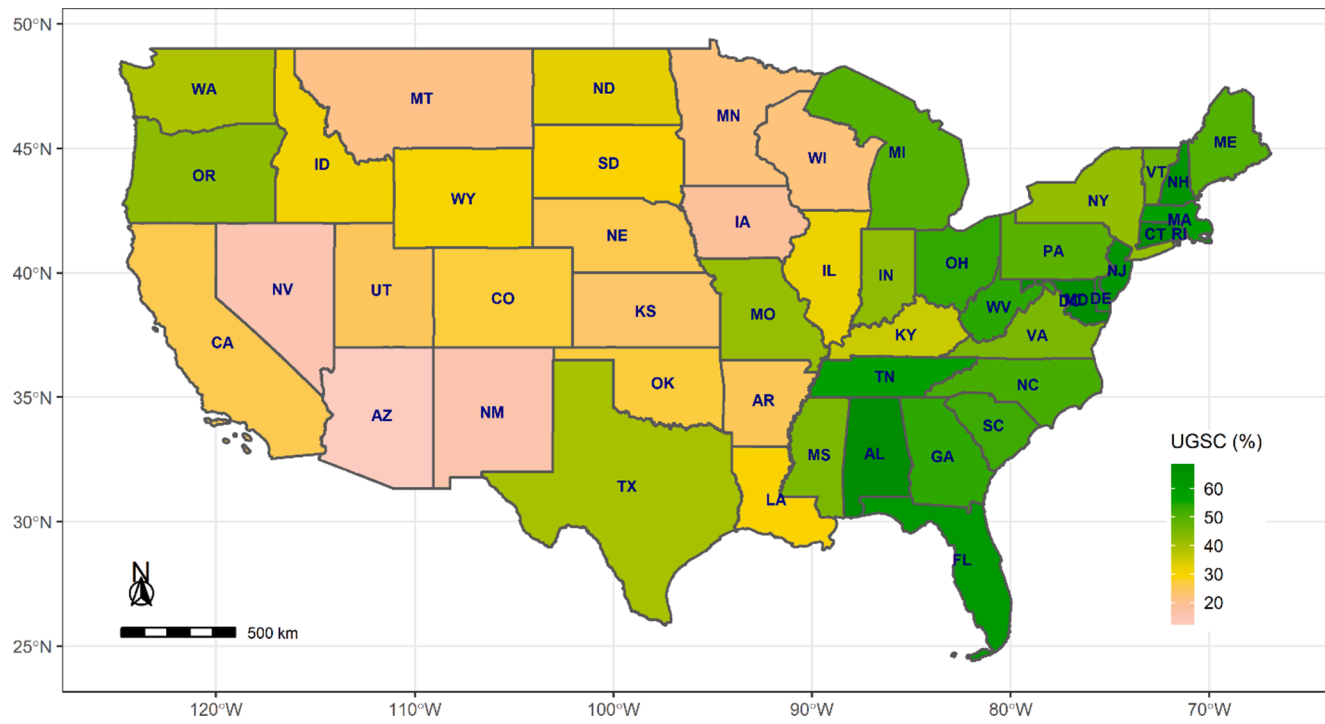


Fig. 5. Spatial pattern of urban green space coverage (UGSC, %) of urban areas aggregated by states.

3.2. Influencing factors of spatial patterns of urban green space coverage

The RF model was constructed to quantitatively investigate the impact of different natural and socio-economic variables on UGSC variation. The result shows that the RF model can explain 73.23% of the UGSC variation in total and we achieved a CV R² of 0.7268, which indicated a good model performance. Fig. 7 shows the relative importance of each influencing factor. The precipitation related variables have

the largest impact on UGSC variation, while areas of each urban area and total population have relatively small influences on UGSC variation (Fig. 7a). After summarizing the influencing factors into three types (i.e., climatic, socio-economic and terrain), it shows that climatic factors have dominant impacts on UGSC variation (Fig. 7b). Among the climatic variables, the precipitation of the driest quarter variable has the largest relative importance (9.9%).

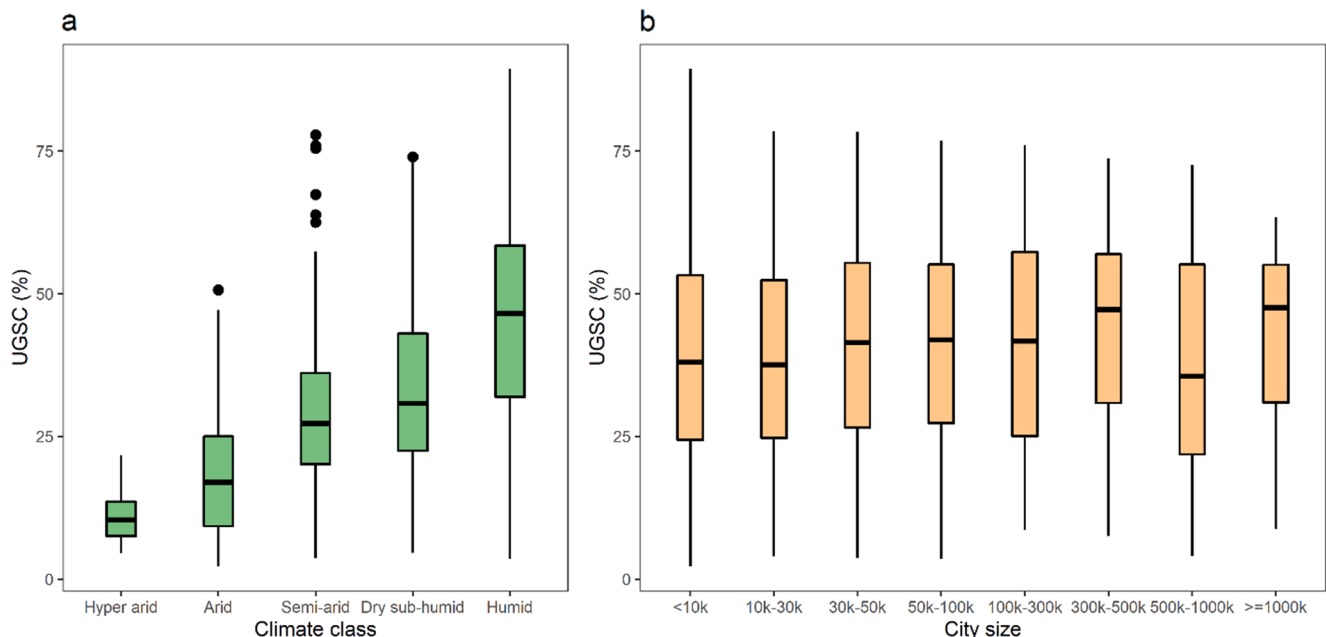


Fig. 6. Boxplots of urban green space coverage (UGSC, %) grouped by climate class (a) and city size (b).

4. Discussion

4.1. Urban green spaces mapped from high-resolution remotely sensed imagery

In this study, we mapped the UGS cover of all the urban areas in the CONUS using one-meter high-resolution remote sensing images, and our study filled the gap of high-resolution UGS cover maps for all the urban areas in the CONUS (Nowak and Greenfield, 2012, 2018). There are also few studies mapping UGS of all their cities at the country scale with such high-resolution images and we highlighted the unique advantage of the use of high-resolution (i.e., one meter) remotely sensed imagery in mapping urban green spaces at large scales (e.g., national scales). Therefore, our high-resolution UGS mapping results could exactly contribute to the field of UGS cover mapping.

In addition, high-resolution UGS maps could be better delineated compared with the results from 30-m resolution Landsat images. As urban landscapes are usually very spatially heterogeneous (Chen and Jim, 2010), medium resolution satellite images can encounter mixed pixels problems (Li, 2017). Vegetation, impervious surfaces, and water bodies might be mixed in one pixel of medium resolution satellite images, making it challenging to map the UGS accurately. The high-resolution remote sensing images can overcome this shortage and better differentiate UGS from other adjacent land cover types (e.g., impervious surfaces). Fig. 8 gives an example of mapping results of this study using 1-meter high-resolution remotely sensed imagery and the National Land Cover Database (NLCD) of the US (Yang et al., 2018) that uses the 30-meter Landsat satellite images. From Fig. 8, we can clearly see that many UGS with small patch sizes are missed due to the coarse spatial resolution.

4.2. Spatial patterns and influencing factors of urban green space coverage

We estimated UGSC with the generated high-resolution UGS maps and analyzed the spatial patterns of UGSC in urban areas of the CONUS. Our results revealed that UGSC varied greatly among urban areas with different states and climate classes. UGSC in humid Eastern US was much higher than that in urban areas with hyper-arid or arid climates in Western or Central regions of the US. Yet, we found that in terms of total

populations of urban areas, UGSC of urban areas with different city sizes does not vary largely from those of urban areas with different climate classes. The UGSC patterns among climate classes are similar to a recent study on UGSC patterns for large- and medium-sized global cities (Huang et al., 2021b). They also found that the UGSC of cities in arid and semi-arid desert biome was much lower than UGSC of cities in other biome types. The potential reason for the small variations of UGSC exist among urban areas of different city sizes might be that land-use patterns of the urban areas with different city sizes were similar. The US urban areas usually consist of commerce, industry, housing, or residential and other lands, of which housing or residential land accounts for the majority (White and Engelen, 1993). The UGS of residential areas usually contain street trees and lawns, and the patterns are similar among urban areas with different city sizes. The similar greening patterns of residential areas in urban areas of varying city sizes might then result in small variations of UGSC in these urban areas.

According to the RF regression analysis, the climatic factors dominate the spatial patterns of UGSC in urban areas of the CONUS, while the socio-economic and terrain factors play relatively less important roles in shaping the UGSC patterns. The finding reflects that climate conditions (e.g., precipitation or water availability) play key roles in vegetation distribution patterns in both natural and urban ecosystems (Nowak et al., 1996; Stephenson, 1990). It also could well explain the significant difference of UGSC in urban areas with different climate classes in the CONUS. Moreover, the potential reason that socio-economic factors play a less important role in shaping the UGSC patterns might be that the economic condition is not a limiting factor of urban greening in these urban areas. In other words, socio-economic conditions in most urban areas of the US do not vary largely because it is one of the most developed countries.

4.3. Implications

The high-resolution UGS mapping results can contribute to the research communities and land management related policy-makers. For example, using the generated UGS maps, UGS exposures or UGS accessibility of each urban area can be further estimated. The UGS exposure information could be then linked to many health indicators to explore the health effects of UGS exposure. Rather than using the medium resolution NDVI as an indicator of greenness (Brown et al., 2018; Yeager

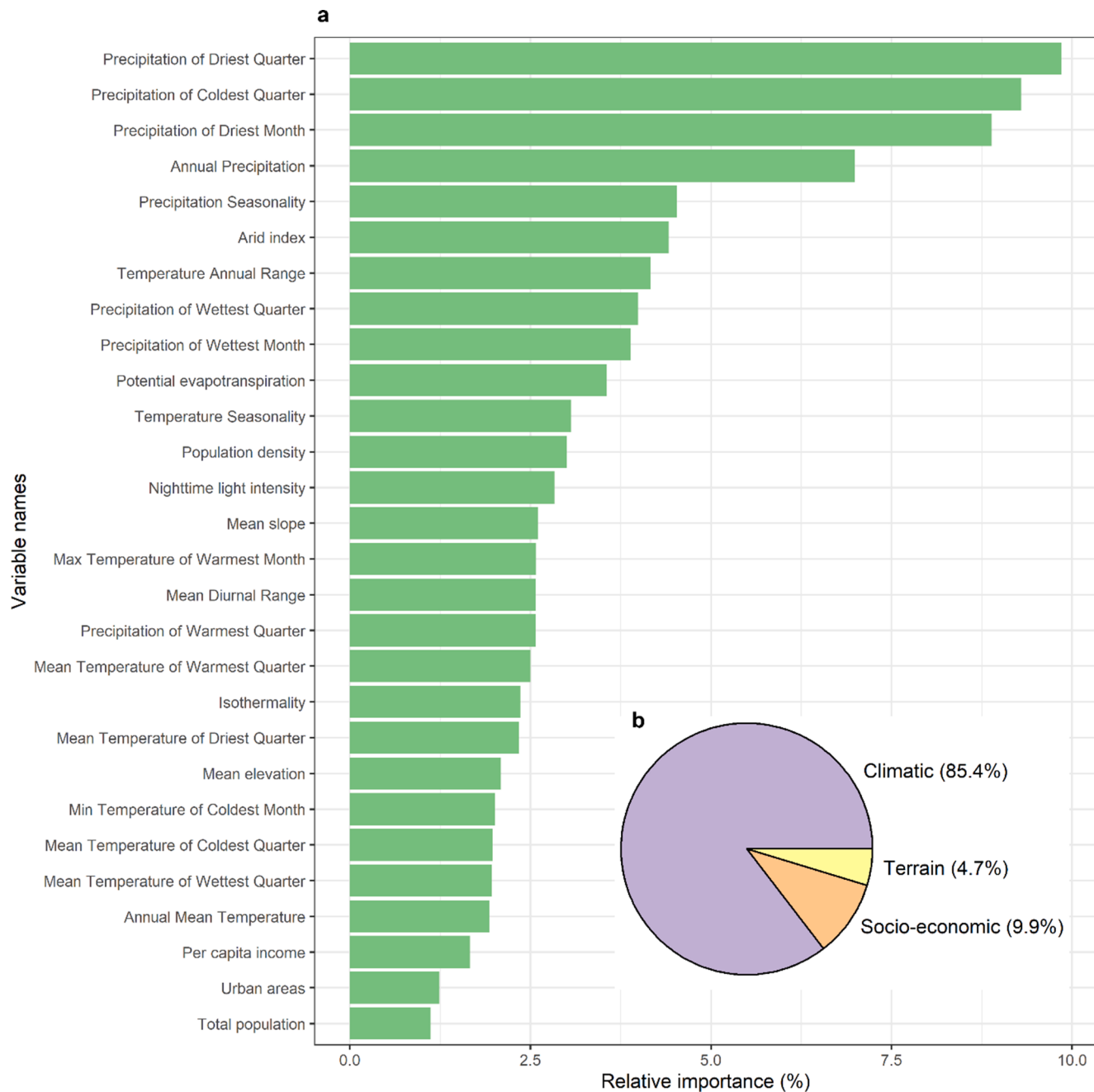


Fig. 7. The relative importance of variables affecting urban green space coverage in urban areas of the contiguous United States.

et al., 2018), our mapping results could provide direct maps of UGS and more detailed information on UGS (e.g., UGS patch size, patch density, etc.). The findings of this study on spatial patterns of UGSC in the CONUS and their shaping influencing factors could provide supporting information for UGS planning and urban sustainable development. For example, it is found that the water deficient areas in the Western US had a decreasing trend of surface water body area from 1984 to 2016 (Zou et al., 2018), thus urban areas in these regions may face increased water stress in the future. Another example is that California has experienced severe drought in recent years (Luković et al., 2021), thus these areas tend to face high water stresses. As a result, it needs a focus on water pressure in future planning for the policy-makers in these areas.

5. Conclusions

This study mapped UGS cover of all the 3,535 urban areas of the

CONUS using the one-meter high-resolution remote sensing images from the NAIP on GEE platform. Using the generated UGS maps of each urban areas, we revealed the spatial patterns of UGSC in these urban areas. We found that UGSC in humid Eastern US was much higher than that in urban areas with hyper-arid or arid climate in Western or Central regions of the US, while the UGSC of urban areas with different city sizes in terms of the total population does not vary largely compared with UGSC of urban areas in different climate classes. We established an RF regression model to investigate the influencing factors of the spatial pattern of UGSC in these urban areas. We found that the climatic factors dominate the spatial patterns of UGSC in urban areas of the CONUS, while the socio-economic and terrain factors play relatively less important roles in shaping the UGSC pattern. We highlighted the advantage of the use of one-meter high-resolution remotely sensed imagery in mapping national-scale urban green spaces, and our UGS mapping results and findings could provide fundamental information for

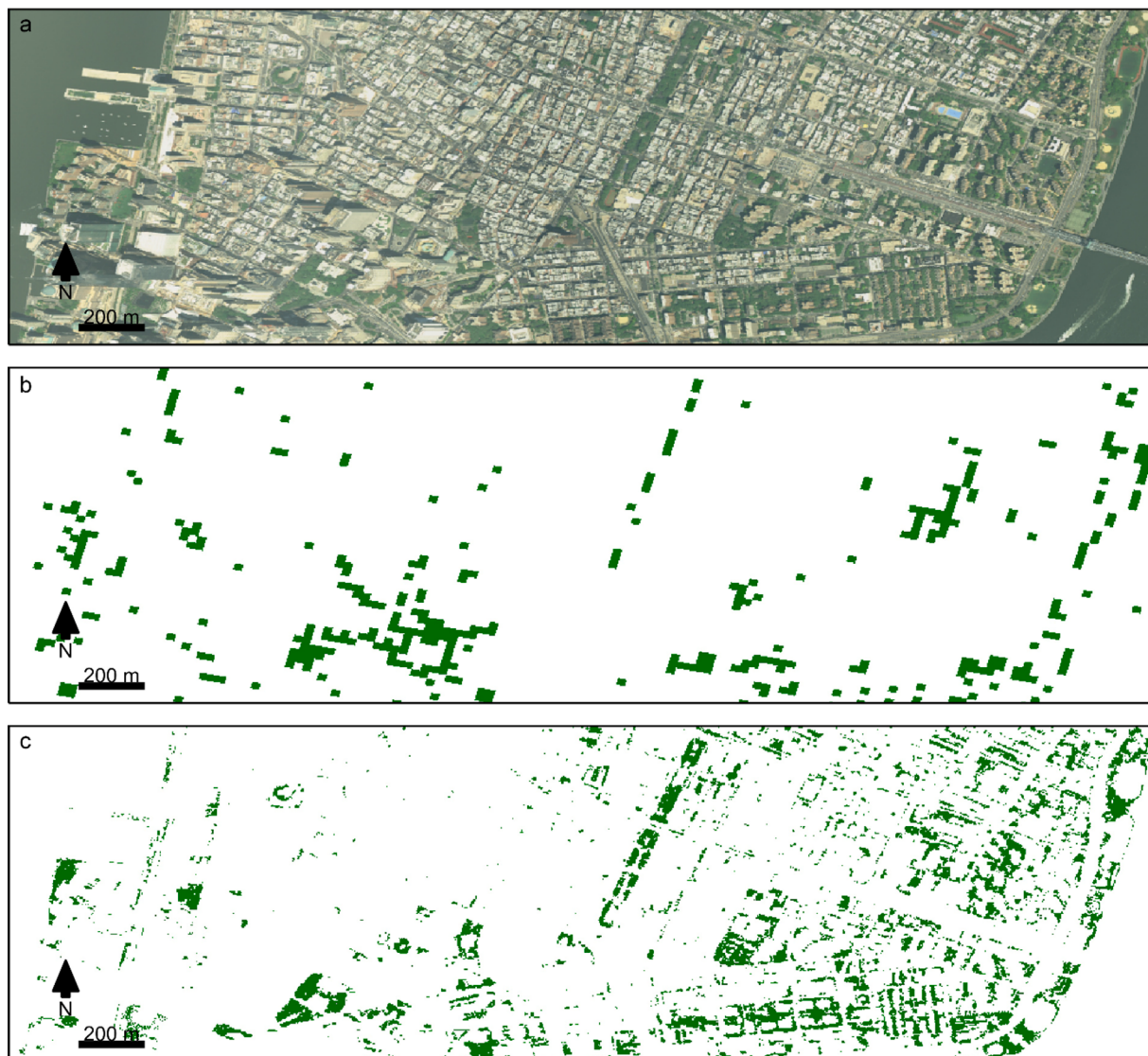


Fig. 8. Illustration of high-resolution remotely sensed imagery and urban green space cover maps in a selected area of the New York-Newark urban area. (a) high-resolution remotely sensed imagery. (b) urban green space cover derived from the National Land Cover Database (merging the forest, shrubland, herbaceous, and developed open space). (c) urban green spaces cover generated in this study.

supporting UGS planning and urban sustainable development.

CRediT authorship contribution statement

Conghong Huang: Conceptualization, Methodology, Software, Writing – original draft. **Nan Xu:** Methodology, Data curation, Writing – review & editing.

Declaration of Competing Interest

The authors declare that they have no known competing financial interests or personal relationships that could have appeared to influence the work reported in this paper.

Acknowledgments

We thank the Google Earth Engine platform for providing us remote sensing data processing platform and online storage. We thank the three anonymous reviewers for their insightful comments. We thank Chao Wu from University of Utah for his comments on the manuscript. This study was supported by the Jiangsu Innovation and Entrepreneurship Program

[184080H10827]. The authors declare no competing financial interest.

References

- Astell-Burt, T., Navakatikyan, M.A., Walsan, R., Davis, W., Figtree, G., Arnolda, L., Feng, X., 2021. Green space and cardiovascular health in people with type 2 diabetes. *Health & Place* 69, 102554.
- Bauwelinck, M., Casas, L., Nawrot, T.S., Nemery, B., Trabelsi, S., Thomas, I., Aerts, R., Lefebvre, W., Vanpoucke, C., Van Nieuwenhuyse, A., 2021. Residing in urban areas with higher green space is associated with lower mortality risk: A census-based cohort study with ten years of follow-up. *Environ. Int.* 148, 106365.
- Breiman, L., 2001. Random forests. *Mach. Learning* 45, 5–32.
- Brown, S.C., Perrino, T., Lombard, J., Wang, K., Toro, M., Rundek, T., Gutierrez, C.M., Dong, C., Plater-Zyberk, E., Nardi, M.I., 2018. Health disparities in the relationship of neighborhood greenness to mental health outcomes in 249,405 US Medicare beneficiaries. *Int. J. Environ. Res. Public Health* 15, 430.
- Chen, W.Y., Jim, C.Y., 2010. Amenities and disamenities: A hedonic analysis of the heterogeneous urban landscape in Shenzhen (China). *Geogr. J.* 176, 227–240.
- Corbane, C., Martino, P., Panagiotis, P., Aneta, F.J., Michele, M., Sergio, F., Marcello, S., Daniele, E., Gustavo, N., Thomas, K., 2020. The grey-green divide: multi-temporal analysis of greenness across 10,000 urban centres derived from the Global Human Settlement Layer (GHSL). *Int. J. Digital Earth* 13, 101–118.
- Dobbs, C., Nitschke, C., Kendal, D., 2017. Assessing the drivers shaping global patterns of urban vegetation landscape structure. *Sci. Total Environ.* 592, 171–177.
- Fick, S.E., Hijmans, R.J., 2017. WorldClim 2: new 1-km spatial resolution climate surfaces for global land areas. *Int. J. Climatol.* 37, 4302–4315.

- Fuller, R.A., Gaston, K.J., 2009. The scaling of green space coverage in European cities. *Biol. Lett.* 5, 352–355.
- Gorelick, N., Hancher, M., Dixon, M., Ilyushchenko, S., Thau, D., Moore, R., 2017. Google Earth Engine: Planetary-scale geospatial analysis for everyone. *Remote Sens. Environ.* 202, 18–27.
- Hashim, H., Abd Latif, Z., Adnan, N.A., 2019. Urban vegetation classification with NDVI thresholds value method with very high resolution (VHR) PLEIADES Imagery. *Int. Arch. Photogramm. Remote Sens. Spat. Inf. Sci.* 237–240.
- Huang, C., Hu, J., Xue, T., Xu, H., Wang, M., 2021a. High-resolution spatiotemporal modeling for ambient PM_{2.5} exposure assessment in China from 2013 to 2019. *Environ. Sci. Technol.* 55, 2152–2162.
- Huang, C., Yang, J., Clinton, N., Yu, L., Huang, H., Dronova, I., Jin, J., 2021b. Mapping the maximum extents of urban green spaces in 1039 cities using dense satellite images. *Environ. Res. Lett.* 16, 064072.
- Huang, C., Yang, J., Lu, H., Huang, H., Yu, L., 2017. Green spaces as an indicator of urban health: evaluating its changes in 28 mega-cities. *Remote Sens.* 9, 1266.
- Hystad, P., Payette, Y., Noisel, N., Boileau, C., 2019. Green space associations with mental health and cognitive function: results from the Quebec CARTaGENE cohort. *Environ. Epidemiol.* 3.
- Jarvis, A., Reuter, H.I., Nelson, A., Guevara, E., 2008. Hole-filled SRTM for the globe Version 4. available from the CGIAR-CSI SRTM 90m Database (<http://srtm.csi.cgiar.org>) 15, 25–54.
- Jarvis, I., Koehoorn, M., Gergel, S.E., van den Bosch, M., 2020. Different types of urban natural environments influence various dimensions of self-reported health. *Environ. Res.* 186, 109614.
- Jaung, W., Carrasco, L.R., Shaikh, S.F.E.A., Tan, P.Y., Richards, D.R., 2020. Temperature and air pollution reductions by urban green spaces are highly valued in a tropical city-state. *Urban For. Urban Greening* 55, 126827.
- Kuang, W., 2019. Mapping global impervious surface area and green space within urban environments. *Sci. China Earth Sci.* 62.
- Kuklina, V., Sizov, O., Fedorov, R., 2021. Green spaces as an indicator of urban sustainability in the Arctic cities: Case of Nadym. *Polar Sci.* 100672.
- Li, W., 2017. Examining the importance of endmember class and spectra variability in unmixing analysis for mapping urban impervious surfaces. *Adv. Space Res.* 60, 2389–2401.
- Luković, J., Chiang, J.C., Blagojević, D., Sekulić, A., 2021. A later onset of the rainy season in California. *Geophys. Res. Lett.* 48, e2020GL090350.
- Massoni, E.S., Barton, D.N., Rusch, G.M., Gundersen, V., 2018. Bigger, more diverse and better? Mapping structural diversity and its recreational value in urban green spaces. *Ecosyst. Serv.* 31, 502–516.
- Mills, S., Weiss, S., Liang, C., 2013. VIIRS day/night band (DNB) stray light characterization and correction, Earth Observing Systems XVIII. International Society for Optics and Photonics, p. 88661P.
- Nowak, D.J., Greenfield, E.J., 2012. Tree and impervious cover change in US cities. *Urban For. Urban Greening* 11, 21–30.
- Nowak, D.J., Greenfield, E.J., 2018. Declining urban and community tree cover in the United States. *Urban For. Urban Greening* 32, 32–55.
- Nowak, D.J., Rowntree, R.A., McPherson, E.G., Sisinni, S.M., Kerkmann, E.R., Stevens, J. C., 1996. Measuring and analyzing urban tree cover. *Landscape Urban Plann.* 36, 49–57.
- Pekel, J.-F., Cottam, A., Gorelick, N., Belward, A.S., 2016. High-resolution mapping of global surface water and its long-term changes. *Nature* 540, 418–422.
- Qian, Y., Zhou, W., Yu, W., Pickett, S.T., 2015. Quantifying spatiotemporal pattern of urban greenspace: new insights from high resolution data. *Landscape Ecol.* 30, 1165–1173.
- Reid, C.E., Clougherty, J.E., Shmool, J.L., Kubzansky, L.D., 2017. Is all urban green space the same? A comparison of the health benefits of trees and grass in New York City. *Int. J. Environ. Res. Public Health* 14, 1411.
- Richards, D.R., Belcher, R.N., 2020. Global changes in urban vegetation cover. *Remote Sens.* 12, 23.
- Schug, F., Frantz, D., Okujeni, A., van Der Linden, S., Hostert, P., 2020. Mapping urban-rural gradients of settlements and vegetation at national scale using Sentinel-2 spectral-temporal metrics and regression-based unmixing with synthetic training data. *Remote Sens. Environ.* 246, 111810.
- Sebastiani, A., Marando, F., Manes, F., 2021. Mismatch of regulating ecosystem services for sustainable urban planning: PM₁₀ removal and urban heat island effect mitigation in the municipality of Rome (Italy). *Urban For. Urban Greening* 57, 126938.
- Spadoni, G.L., Cavalli, A., Congedo, L., Munafò, M., 2020. Analysis of Normalized Difference Vegetation Index (NDVI) multi-temporal series for the production of forest cartography. *Remote Sens. Appl.: Soc. Environ.* 20, 100419.
- Stephenson, N.L., 1990. Climatic control of vegetation distribution: the role of the water balance. *Am. Nat.* 135, 649–670.
- Sulma, S., Yulianto, F., Nugroho, J.T., Sofan, P., 2016. A support vector machine object based image analysis approach on urban green space extraction using Pleiades-1A imagery. *Modeling Earth Syst. Environ.* 2, 54.
- Trabucco, A., Zomer, R.J., 2018. Global aridity index and potential evapotranspiration (ETO) climate database v2. CGIAR Consort Spat Inf 10.
- Tucker, C.J., 1979. Red and photographic infrared linear combinations for monitoring vegetation. *Remote Sens. Environ.* 8, 127–150.
- Vigneshwaran, S., Vasanth Kumar, S., 2019. Comparison of classification methods for urban green space extraction using very high resolution worldview-3 imagery. *Geocarto Int.* 1–14.
- White, R., Engelen, G., 1993. Cellular automata and fractal urban form: a cellular modelling approach to the evolution of urban land-use patterns. *Environ. Planning A* 25, 1175–1199.
- Wright, M.N., Ziegler, A., 2017. Ranger: A fast implementation of random forests for high dimensional data in C++ and R. *J. Stat. Softw.* 77.
- Yang, J., Huang, C., Zhang, Z., Wang, L., 2014. The temporal trend of urban green coverage in major Chinese cities between 1990 and 2010. *Urban For. Urban Greening* 13, 19–27.
- Yang, L., Jin, S., Danielson, P., Homer, C., Gass, L., Bender, S.M., Case, A., Costello, C., Dewitz, J., Fry, J., 2018. A new generation of the United States National Land Cover Database: Requirements, research priorities, design, and implementation strategies. *ISPRS J. Photogramm. Remote Sens.* 146, 108–123.
- Yeager, R., Riggs, D.W., DeJarnett, N., Tollerud, D.J., Wilson, J., Conklin, D.J., O'Toole, T.E., McCracken, J., Lorkiewicz, P., Xie, Z., 2018. Association between residential greenness and cardiovascular disease risk. *J. Am. Heart Assoc.* 7, e009117.
- Zhao, J., Chen, S., Jiang, B., Ren, Y., Wang, H., Vause, J., Yu, H., 2013. Temporal trend of green space coverage in China and its relationship with urbanization over the last two decades. *Sci. Total Environ.* 442, 455–465.
- Zhou, W., Wang, J., Qian, Y., Pickett, S.T., Li, W., Han, L., 2018. The rapid but “invisible” changes in urban greenspace: A comparative study of nine Chinese cities. *Sci. Total Environ.* 627, 1572–1584.
- Zomer, R.J., Trabucco, A., Bossio, D.A., Verchot, L.V., 2008. Climate change mitigation: A spatial analysis of global land suitability for clean development mechanism afforestation and reforestation. *Agric. Ecosyst. Environ.* 126, 67–80.
- Zou, Z., Xiao, X., Dong, J., Qin, Y., Doughty, R.B., Menarguez, M.A., Zhang, G., Wang, J., 2018. Divergent trends of open-surface water body area in the contiguous United States from 1984 to 2016. *Proc. Natl. Acad. Sci.* 115, 3810–3815.